J. Fluid Mech. (1979), *vol.* 95, *part* 1, *pp.* 79–96
Printed in Great Britain

The diffraction of a planar detonation wave at an abrupt area change

By D. H. EDWARDS, G. O. THOMAS
Department of Physics, University College of Wales, Aberystwyth
AND M. A. NETTLETON
Central Electricity Research Laboratories, Leatherhead

(Received 29 November 1978)

Previous experimental work on the diffraction of a detonation wave at a large and abrupt area change in a tube, has shown that every system is characterized by a critical tube diameter at which quenching of the detonation occurs. Zeldovich, Kogarko & Simonov (1956) established that the critical tube diameter, for the oxy-acetylene system with varying dilution of nitrogen, lies between 500 and 700 times the one-dimensional induction zone length. Later, Mitrovanov & Soloukhin (1964) discovered that, for the same system, the critical diameter is 10 or 13 times the transverse wave spacing for a flat channel and cylindrical tube respectively. The two results are shown to be equivalent and are confirmed by further experiments in a 75×6 mm channel in which the flow is two-dimensional.

Smoked foil and schlieren records show that, for supercritical waves, re-ignition occurs at sites along the wedge formed by the head of the expansion from the diffracting aperture and criticality is attained when the site is located at the apex of the wedge. A universal feature of re-initiation, which is also observed in liquid and solid explosives, is the sudden appearance of a transverse detonation which sweeps through the compressed, but unreacted, gas of the dissociated shock-reaction zone regime; this is signalled by the appearance of fine triple-point writing on smoked-foil records.

A criterion for re-initiation is formulated by equating the critical velocity gradient which characterizes the decay of the wavefront in a cell, to that obtaining in the diffracted shock front at the head of the expansion fan; an expression for the latter is derived from Whitham's (1957) theory for non-reactive shocks. The prediction of the criterion is in good agreement with observation.

1. Introduction

The global properties of a self-sustaining detonation wave are adequately described by the one-dimensional Chapman–Jouguet (CJ) model, in which a plane shock front initiates chemical reaction and, further downstream, at a parallel plane, thermodynamic equilibrium obtains and the particle velocity is sonic relative to the front. For waves near the limits of detonability, or when subjected to large perturbations, the inadequacies of the CJ model manifest themselves. Under these circumstances cognizance must be taken of the non-steady three-dimensional frontal structure in describing the wave behaviour. This structure, which is a feature of all self-propagating waves, is the result of the complex interaction of the gasdynamics and chemical

0022-1120/79/4312-7430 $02.00

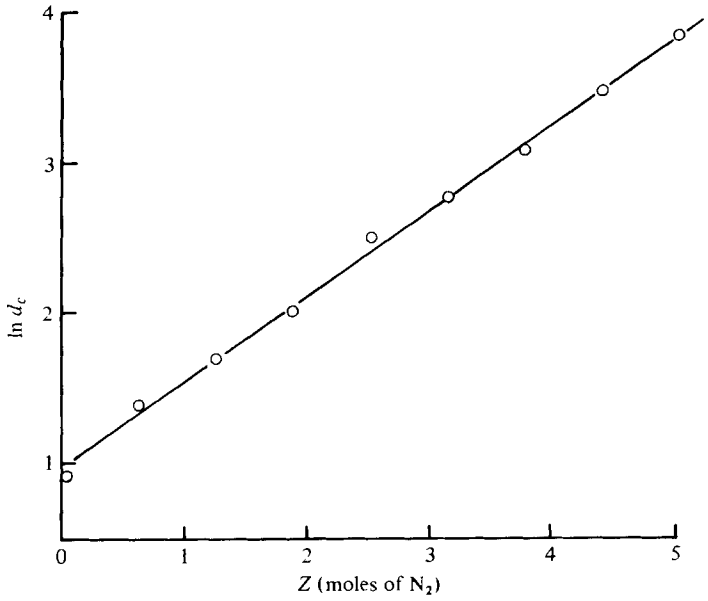

FIGURE 1. Experimental observations of Zeldovich *et al.* (1956) on the dependence of critical tube diameter d_c on Z in $C_2H_2+O_2+ZN_2$ at an initial pressure of 800 Torr.

kinetics and the spatial extent of this interaction, sometimes termed the 'gasdynamic thickness' of the wave, is roughly an order of magnitude greater than the chemical reaction zone thickness.

A problem which exemplifies the importance of considerations of wavefront structure in its solution, is that of the transition of a planar detonation into a spherical or cylindrical one. This problem has attracted much attention in recent years, both for its fundamental and practical interest. Such a phenomenon arises when a wave propagating in a tube meets with an abrupt area change: under certain circumstances the expansion causes the detonation to be quenched while others permit re-establishment to occur. This observed behaviour is not unique to the gas phase but is a problem which is common equally to solid- and liquid-phase detonation, as shown by Dremin & Trofimov (1965). They arrived at the important conclusion that the critical diameter of a weakly confined solid or liquid explosive corresponds to the quenching diameter of a detonation wave passing into a larger volume of explosive. They argued that this coincidence of critical diameter values is not fortuitous and that previous theories of critical explosive diameters of unconfined charges, which assume that quenching results when rarefaction waves from the charge periphery reach the charge axis before the completion of reaction, are essentially incorrect because they ignore the influence of frontal structure. A rudimentary fluid-dynamic analysis of the problem is proposed, based on the observation of oblique frontal waves, which, it is claimed, gives better agreement with experimental data. More recently, Urtiew (1975) has adduced further evidence of the cellular structure in liquid explosives, similar to that found in gaseous detonations. Moreover, he was able to explain the origin and growth of failure waves in unconfined explosives on the basis of the transverse motion and reflection of the triple-wave intersections that are present in cellular structures. The relevance of these theories to the present results is discussed in § 6.

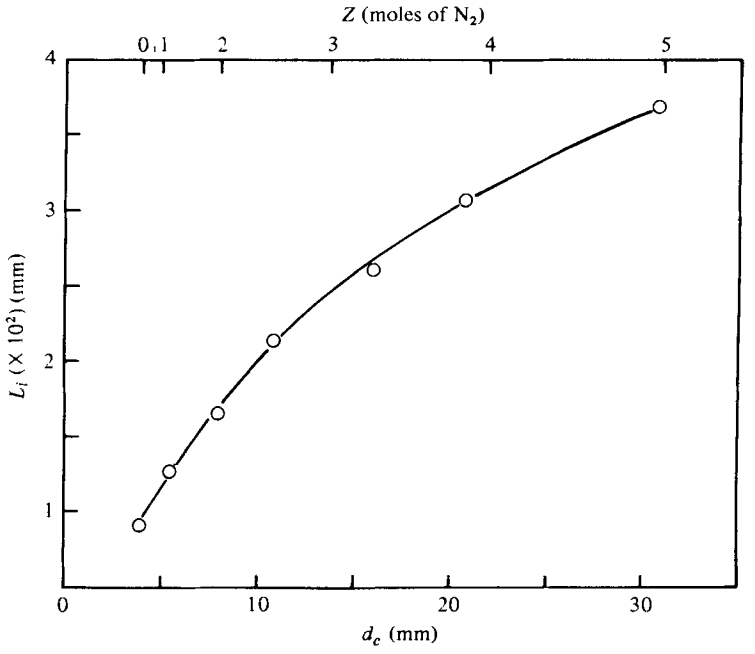

FIGURE 2. Dependence of one-dimensional induction zone thickness L_i on critical diameter d_c derived from the data of Zeldovich *et al.* given in figure 1.

In their classic paper on an experimental investigation of spherical detonations in gases, Zeldovich, Kogarko & Simonov (1956) examined the behaviour of a detonation wave as it emerged from a narrow channel into a larger one. Prior to this study the information available on this transition, and indeed on the initiation of spherical detonation generally, was scant. These authors employed a total of 14 gas mixtures at an initial pressure of 800 Torr, and a range of tubes, of circular section, with diameters from 2 to 33 mm. They concluded that each mixture is characterized by a critical tube diameter d_c for which spherical detonation was only just initiated in the larger-diameter tube. The relationship between the experimental values of d_c and the degree of dilution of each system was established; this is given in figure 1 for the oxyacetylene–nitrogen compositions only, since we shall restrict our attention to these in the present study. The relationship was found to be

$$\ln d_c = 0{\cdot}57Z + 0{\cdot}99, \tag{1}$$

where Z is the ratio of the number of moles of nitrogen to that of stoichiometric oxyacetylene. Furthermore, they found that d_c, in all the systems studied, was related to the induction zone length L_i by the expression

$$d_c/L_i \simeq 15. \tag{2}$$

Here, L_i is defined as the distance between the plane causal shock in a one-dimensional wave and the onset of the zone of exothermic release. If τ_i is the one-dimensional steady-state induction reaction time, then $L_i = \tau_i M_s a_0$, where M_s is the shock Mach number and a_0 the speed of sound in the mixture. We have recomputed L_i for the oxyacetylene data quoted above using more reliable values of τ_i than were available

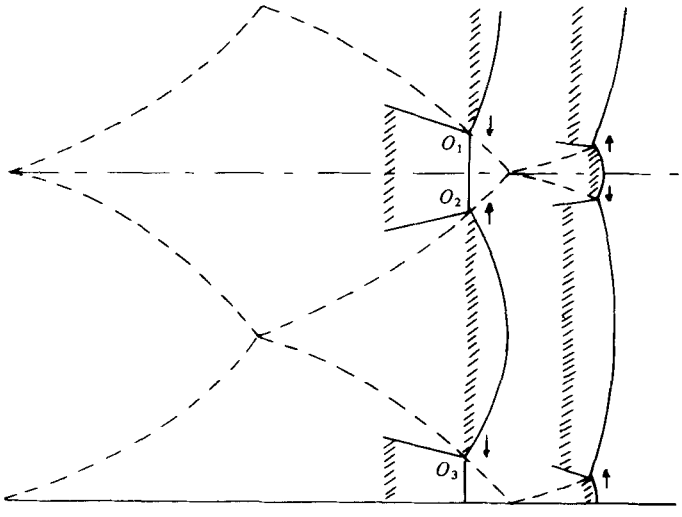

FIGURE 3. Sketch of detonation wavefront showing triple-wave intersection just before and immediately after reflexion at a rigid wall and the same between two symmetric waves of the opposite family. Hatching denotes reaction zone and dotted lines the smoked-foil traces of the triple points.

to Zeldovich *et al.*, and found (2) to be in error. Values of τ_i were derived from (3) given by White (1967):

$$\log_{10}\{[O_2]^{\frac{1}{3}}[C_2H_2]^{\frac{2}{3}}\tau_i\} = -10{\cdot}81 + 17\,300/4{\cdot}58T. \tag{3}$$

The experimental values of d_c and calculated values of L_i are plotted in figure 2. Thus for

$$2 < d_c \lesssim 15 \text{ mm}, \quad \text{we have} \quad d_c/L_i \approx 500,$$

and for

$$d_c \gtrsim 15 \text{ mm}, \quad \text{we have} \quad d_c/L_i \approx 700. \tag{4}$$

These values are an order of magnitude greater than those given by Zeldovich *et al.* in (2) and, moreover, the dependence of d_c on L_i is not linear over the whole range of Z values.

The next significant attempts to understand the diffraction of a detonation wave at the exit of a tube were those of Gvozdeva (1961) and Mitrovanov & Soloukhin (1964). The latter authors kept the tube diameter constant and varied L_i by changing the initial pressure of a stoichiometric oxyacetylene mixture. They discovered a fundamentally important result which relates the critical diameter to the equilibrium transverse wave spacing S:

$$d_c = 13S \quad \text{for a circular tube;} \quad d_c = 10S \quad \text{for a planar channel.} \tag{5}$$

Figure 3 is a sketch of the wavefront in a planar detonation, showing the relative dispositions of the frontal and transverse shocks and the exothermic reaction zones. The trajectories of the triple points, O_1, O_2, O_3, etc., write characteristic patterns or cells on smoked foil placed on the tube walls, whose transverse and longitudinal dimensions are S and L_c respectively. Cell size varies with the chemical kinetics of the system and thus with composition of the mixture and its initial pressure, but the cell

shape is essentially invariant, with $S \simeq 0{\cdot}6L_c$. There is also a fair amount of evidence (e.g. Vasiliev, Gavrilenko & Topchian, 1972) that L_c is related to L_i by

$$L_c = n \times 10L_i, \tag{6}$$

where $5 \leqslant n \leqslant 10$. Then from (5) and (6)

$$d_c = 13 \times 0{\cdot}6 \times n \times 10L_i = 78nL_i \quad \text{for a circular tube,}$$

and $$d_c = 10 \times 0{\cdot}6 \times n \times 10L_i = 60nL_i \quad \text{for a planar channel.} \tag{7}$$

Bearing in mind the approximate nature of equation (6), equation (7) is in reasonable accord with equation (4), so that the observations of Zeldovich *et al.* and Mitrovanov & Soloukhin are shown to be approximately equivalent. Further experimental evidence of the transition from planar to spherical detonation was described by Soloukhin & Ragland (1969). The detailed behaviour of the expanding wavefront was obtained by spark and streak schlieren photography. They concluded that the ignition process behind the expanding decelerating wave can be separated into three regimes:

(i) multi-front ignition (continuous transition),

(ii) self-ignition associated with localized explosion behind a smooth front (critical transition),

(iii) deflagration behind an entirely separated shock front (failure).

In (ii) the detonation remains unchanged for roughly two tube diameters before the external expansion wave affects it. The velocity then decreases until a localized 'explosion' occurs which sweeps around the new curved front raising the velocity back to the CJ value. For a failing wave this explosion does not occur and the shock becomes smooth with the reaction zone separated from it.

Since transverse waves play a paramount role in detonation wave propagation it would seem that progress could be made in the elucidation of the diffraction process by attempting to relate the strength and spacing of these waves to the flow-field parameters behind the diffracted wavefront. However, as Strehlow & Engel (1969) have shown, the dependence of cell dimensions on the chemical kinetics is a complex one and both reactions in the induction and recombination zones are influential factors. Although much progress has been made in this area by the application of the theory of acoustic wave amplification in reactive flow to the prediction of wave spacings (Strehlow 1970; Barthel 1974), the theory requires a complete description of the particle and sound velocities in the flow field behind a one-dimensional steady shock. It is not clear at present how such an analysis could be applied to the non-steady flow field of the diffracted shock front. Consequently, we shall interpret our observations in terms of an observable L_c and then relate this dimension empirically to a kinetic length L_i as in (6).

The aim of the present work is to enlarge upon the findings of the previous studies discussed above, and in particular to obtain a more detailed description of the mechanism of re-initiation at criticality. On the basis of these results an attempt is made to formulate a criterion for criticality by adopting the theory of the diffraction of a non-reactive shock.

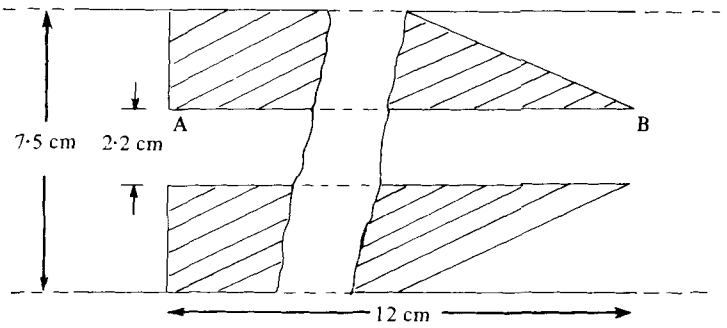

FIGURE 4. Principal dimensions of Tufnol wedge placed in the shock tube to produce the area change.

2. Experimental details

Since schlieren records can be interpreted with far greater confidence in two-dimensional flows than those in three dimensions, it was decided to study the transition process in a rectangular channel rather than a circular-section tube. Moreover, by making the lateral dimensions of the channel very narrow, transverse perturbations in that dimension are substantially reduced. A disadvantage that arises, of course, is the influence of the wall boundary layer on the flow at the low pressures used in the present study. Following Mitrovanov & Soloukhin (1964) we have varied the initial pressure of the gas mixtures while keeping the tube dimensions constant. In this way the influence of varying the kinetics is studied, and consequently L_i and L_c, while the gasdynamic parameters remain fairly constant. The motion of the shock fronts and reaction zones were recorded by both spark and streak photography while the trajectories of the triple-point interactions with the tube wall were obtained from smoked-foil records.

The detonation tube was of rectangular section of internal dimensions 75×6 mm and consisted of three sections: a main section of length 4 m, a smoked-foil section 50 cm long and a 30 cm long optical section. The required area change in the major wall of the tube was achieved by inserting a wedge made of Tufnol as shown in figure 4. Great care had to be taken in sealing the gap between the Tufnol and the walls of the tube so that no leakage could occur between the two. It was found that the 12 cm length of the wedge was wholly adequate to ensure the production of a steady detonation wave in the rectangular channel A and also to prevent any reflected disturbances from the end B arriving at the flow field of interest during the recording time.

3. Experimental results

3.1. *Smoked-foil records*

Four examples of smoked-foil records which were obtained with oxyacetylene at initial pressures of 180, 150, 110 and 60 Torr are given in figure 5 (plate 1). These illustrate the type of pattern which is observed under supercritical, critical and failure conditions. A sketch of the principal features of a supercritical record is shown in figure 6 in which re-initiation is seen to occur along the limiting characteristics AD

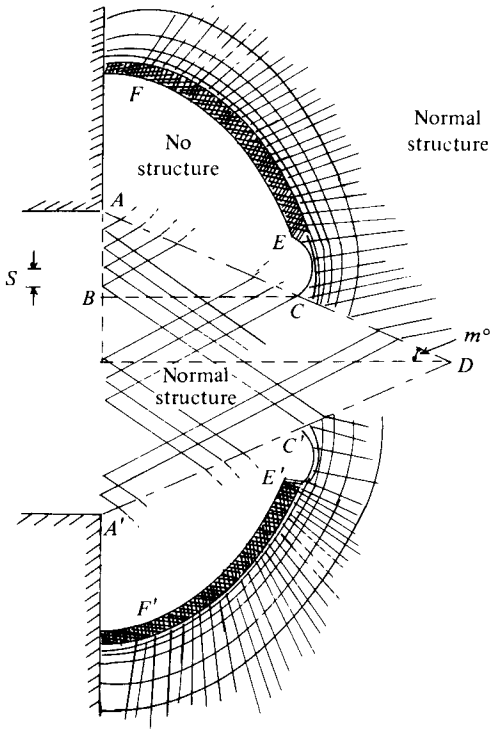

FIGURE 6. Sketch showing essential features of a smoked-foil record obtained under supercritical conditions of re-initiation.

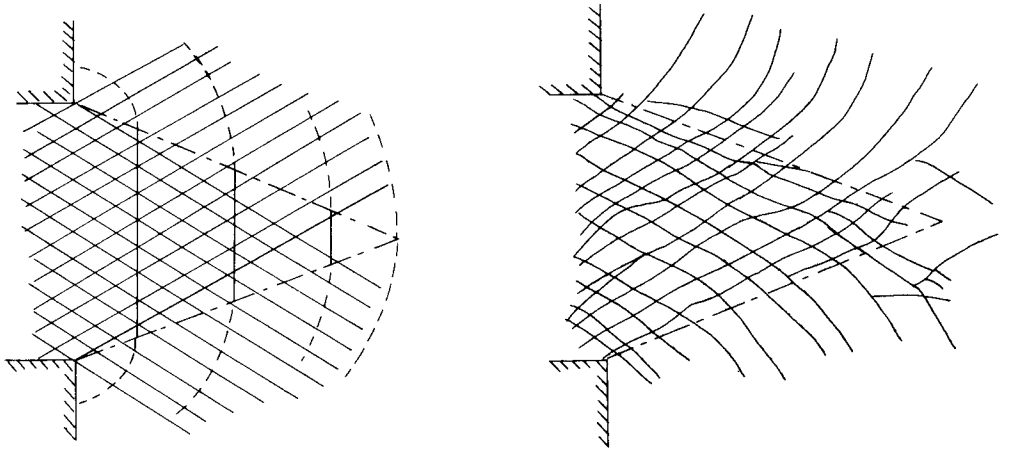

(*a*) (*b*)

FIGURE 7. (*a*) Idealized representation of smoked-foil record at critical conditions and (*b*) tracing of actual record obtained under these conditions.

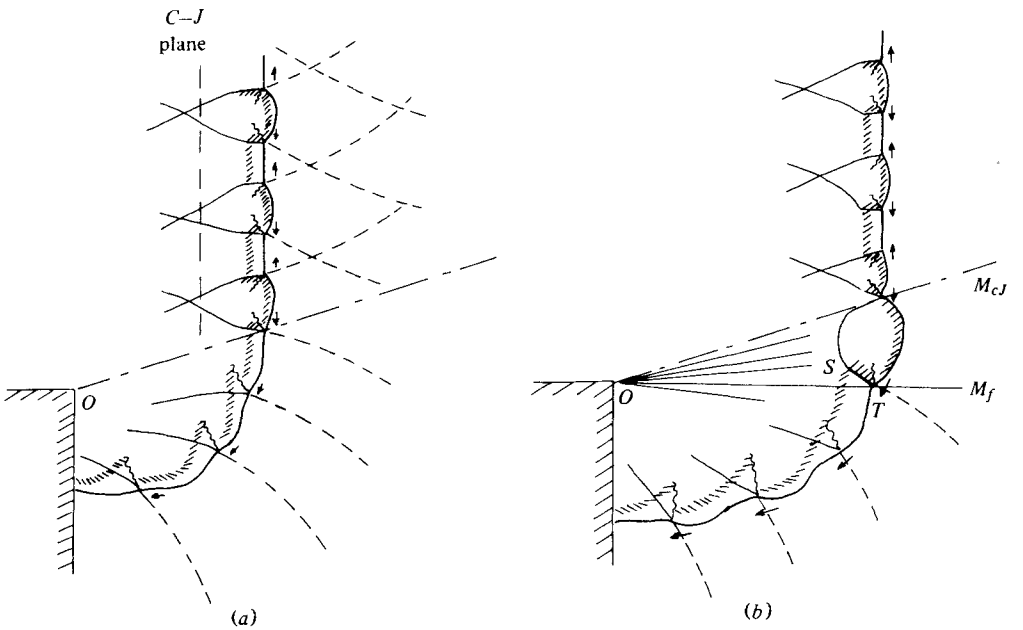

FIGURE 9. Sketch of diffracted detonation front derived from the photographs in figure 8, plate 2. In (*a*) the wavefront is shown just before re-ignition while in (*b*) the transverse detonation TS has been formed. Note that there is no reaction behind the transverse waves in the diffracted portion of the front. Dotted lines represent the trajectories of the triple points.

and $A'D$ at the points C and C'. Re-ignition causes an intense localized blast wave, CE and $C'E'$, to be formed, which propagates both forward into the unburned gas ahead and also as a transverse detonation which sweeps through the shocked, but unreacted gas, between the main front and the decoupled reaction zone. This transverse wave, being an overdrive detonation, gives rise to the very fine triple-point writing along the two arcs EF and $E'F'$. In actual smoked-foil records, however, these arcs are nowhere near as uniform as ideally depicted in the diagram, especially as criticality is approached. As a result of the transverse detonation the main detonation wavefront is temporarily overdriven and thus the cell size in the neighbourhood of the arcs EF and $E'F'$ is smaller than in the normal structure. As the front velocity approaches the CJ value the cells acquire the normal equilibrium size; the cell pattern in this region is not shown in the diagram of figure 6.

At criticality, which is the condition of greatest interest, the re-ignition is delayed to a point in the vicinity of the intersection of the limiting characteristics, D. Figures 7(*a*) and 7(*b*) respectively show the idealized record at criticality and the tracing obtained from an actual foil. One notes that as the transverse waves move out of the region bounded by the expansion wave they are not regenerated by collision with an opposite family of waves.

3.2. *Spark schlieren records*

Examples of spark schlieren records, which correspond to the supercritical, critical and sub-critical regimes referred to in the above section, are shown in figure 8 (plate 2). In record (*a*) the reaction zone is entirely detached from the shock front and, conse-

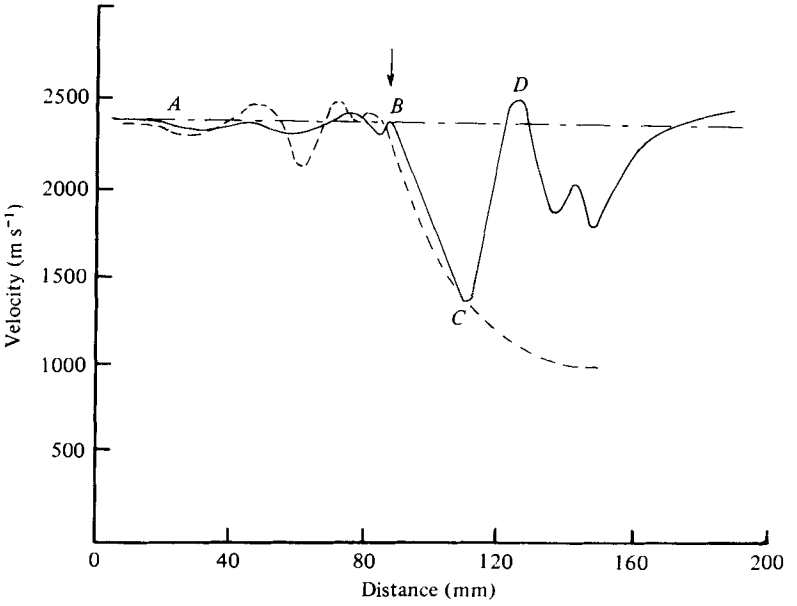

FIGURE 11. Variation of frontal velocity along the axis obtained from streak photographs. Solid line corresponds to critical re-initiation and dashed curve is a failing wave. Arrow denotes position of intersection of expansion heads.

quently, the latter has a fairly smooth appearance because only weak unreactive Mach interactions sweep over its surface. As the wave propagates further from the aperture the shock-reaction zone separation continues to grow and the detonation decays. Records (*b*) and (*c*) show two stages of critical initiation. Re-ignition has occurred in (*b*) at X and X' so that along the front XX' the reaction is closely coupled to the front, whereas, for the remainder of the front XY and $X'Y'$, the reaction and shock front are decoupled as in (*a*). Record (*c*) shows the wavefront of (*b*) at a slightly later time; here the transverse detonation wave at X and X' (labelled TS in figure 9(*b*)) can be seen more clearly. Because a portion of this wave moves into the unreacted gas behind the main front, which is at a high pressure and temperature, it is an overdriven wave and the accompanying triple-points of the Mach interactions give rise to the fine cell writing shown along the trajectories EF and $E'F'$ of figure 6.

Record (*d*) is a photograph of a supercritically initiated wavefront and corresponds to the smoked-foil record of plate 1 at an initial pressure of 180 Torr. The portion labelled XX' is a CJ detonation exhibiting a normal wavefront structure. However, the weakened portions of the diffracted wavefront, XY and $X'Y'$, show a shock-reaction zone detachment as in the other cases, but as the wave propagates further upstream the region XY and $X'Y'$ diminishes in extent and eventually disappears.

A further important feature, present in all the above records, is the weak nature of the transverse waves associated with the triple points in the region where the influence of the expansion is strong. A close examination shows that there is no exothermic reaction behind the transverse waves in this region and the frontal structure corresponds to that sketched in figure 9(*a*). A similar structure is observed in marginal waves of certain systems in detonations propagating in tubes (Subbotin 1974), and it

could well be the type of structure that occurs universally near conditions of wavefront failure.

3.3. *Streak schlieren records*

A continuous record of the behaviour of the wavefront along the axis of symmetry was determined by streak photographs, an example of one being given in figure 10 (plate 3) near critical conditions. The dissociation of the reaction zone followed by re-ignition is clearly observed on these records. Graphs of the shock front velocity near criticality and for failure are plotted in figure 11. These profiles are reminiscent of the behaviour of the front in the ignition of a spherical detonation by a blast wave (Edwards *et al.* 1978; Bull *et al.* 1976). At criticality it is seen that the velocity along the axis is sensibly constant along AB, at the CJ value of 2400 $\mathrm{m\,s^{-1}}$. At B, which is a point just beyond the apex of the wedge formed by the expansion heads, there is a sudden drop in velocity to $0{\cdot}6M_{CJ}$ at C. This is immediately followed by a rapid recovery to a velocity slightly greater than CJ at D. Decay of the front velocity occurs again before a further re-initiation establishes a steady wave.

4. A criterion for critical conditions

In a normal detonation wave the collisions of oppositely moving families of transverse shocks provide the 'ignition sources' which are necessary to sustain the frontal motion. For waves which are confined by solid boundaries the reflexion of transverse waves at the boundaries is clearly important in keeping the average wave spacing constant. In unconfined waves, the transverse collision process must be capable of generating new waves so as to maintain the equilibrium number density appropriate to the system. However, in a diffracted detonation wave the transverse waves moving through the head of the expansion do not meet an opposite family of transverse waves; therefore no new collision centres are formed. Moreover, since the strength of the frontal shock is weakened by the expansion, exothermic reaction ceases to occur behind the transverse shocks. Under these conditions the transverse shock intersections will certainly not generate the new waves which are necessary for the sustenance of the diverging wavefront.

On these two counts, therefore, the shock and reaction zone become separated or dissociated, as can be seen in the schlieren records of figure 10 (plate 2). A sketch of the frontal structure, derived from the photographs, is shown in figure 9 (a) and (b) in which the non-reactive nature of the transverse waves is depicted.

As the wave moves further from the area change the transverse gradient of the Mach number M_s of the diffracted shock, $\partial M_s/\partial y$, becomes less severe until, at a certain distance along the expansion head AD (figure 6), sudden re-ignition occurs. This is followed by the movement of a transversely propagating detonation wave into the pre-compressed gas lying between the frontal shock and dissociated reaction zone. The transverse detonation, TS, is indicated in figure 9 (b) and the characteristic smoke-foil pattern that follows re-initiation in figure 6. The latter figure, as we have noted in § 3.1, is a somewhat idealized representation of the actual smoked-foil records of figure 5 (plate 1 (a) and (b)) because, quite often, re-ignition occurs at more than one site before successful re-establishment of a steady wave. This sometimes gives rise to a rather confused and complicated pattern, particularly as the system approaches

criticality. Nevertheless, figure 6 describes the essential mechanism that is operative. Because the re-establishment of detonation in a diffracted wave is governed by the local value of $\partial M_s/\partial y$ at the expansion head, in any given system, it is required to find the wave parameters which can be related to this gradient at criticality. The obvious mechanism to consider is the progress of a frontal wavelet in a cell, as depicted in figure 13.

The intersection of two transverse waves, of opposite families, creates an overdriven detonative Mach stem at the apex of a new cell. It is well established experimentally that the initial wavefront velocity of the Mach stem is about $1{\cdot}2M_{CJ}$, for systems well removed from the limit, and the terminal value at the end of the cell is $0{\cdot}8M_{CJ}$. An important consequence of this wavefront deceleration is that not all particles entering the front, as it traverses the cell, will succeed in reacting. Kinetic calculations by Thomas (1979) show that only particles entering the wavefront up to a distance of $0{\cdot}35L_c$ from the cell apex will reach the reaction zone; this limit is indicated by A in figure 13. Particles entering at further distances upstream from A will fail to react behind the front and must, therefore, react behind the transverse waves. The reason why a particle entering the front at point B (say) does not react, is that the thermodynamic states along the particle flow path BB' do not allow the induction reaction time τ_i (equation 3) to be realized. At the critical point A the front velocity is approximately M_{CJ}, consequently a maximum value for the velocity decay gradient which leads to shock-reaction front separation, may be expressed as being approximately $0{\cdot}2\,M_{CJ}/L_c$.

An alternative way of establishing the onset of the decoupling of the reaction zone in a decaying wavefront is through the Shchelkin (1959) instability criterion. This semi-qualitative criterion simply states that, for a one-dimensional wavefront, if an increase $\Delta\tau_i$ occurs in the steady-state induction–reaction time τ_i such that

$$\Delta\tau_i/\tau_i \gtrsim 1, \tag{8}$$

then detonation wavefront decays. If τ_i is expressed as

$$\tau_i = A\rho^{-1}\exp(E/RT), \tag{9}$$

where A is a kinetic rate factor, ρ and T the post-shock density and temperature respectively then, by combining (9) with the Rankine–Hugoniot relations for a normal shock wave, one obtains

$$\frac{\Delta\tau_i}{\tau_i} = -2\frac{\Delta M_s}{M_s}\frac{2+(\gamma-1)\,M_s^2\,E/RT}{2+(\gamma-1)\,M_s^2}. \tag{10}$$

Assuming typical values for the activation energy E of 80 kJ mol^{-1}, $T = 2000$ K and $M_s = M_{CJ} = 6$, the inequality (8) becomes

$$\Delta M_{CJ}/M_{CJ} \lesssim -0{\cdot}1. \tag{11}$$

This means that, if the velocity of a plane CJ detonation falls by 10 % below the CJ value, the reaction zone becomes decoupled and the detonation wave decays. Bearing in mind the approximate nature of this calculation we conclude that this result is entirely consistent with the one noted above for the non-steady wavefront in a cell, in which the critical velocity decrease $\Delta M_{CJ}/M_{CJ}$ was observed to be about $-0{\cdot}2$.

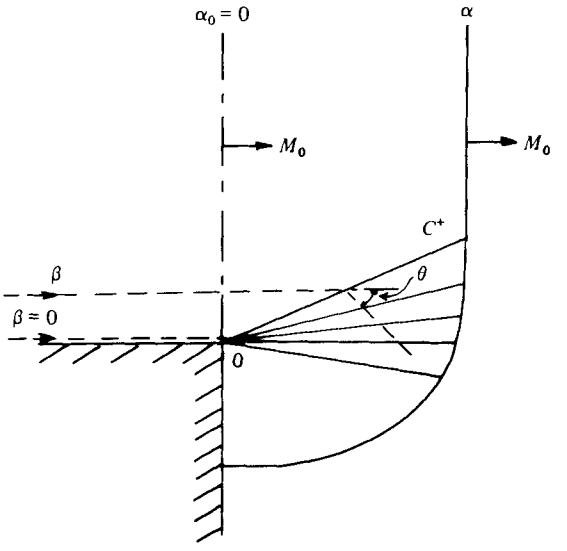

FIGURE 12. Diagram defining the nomenclature used in Whitham's theory.

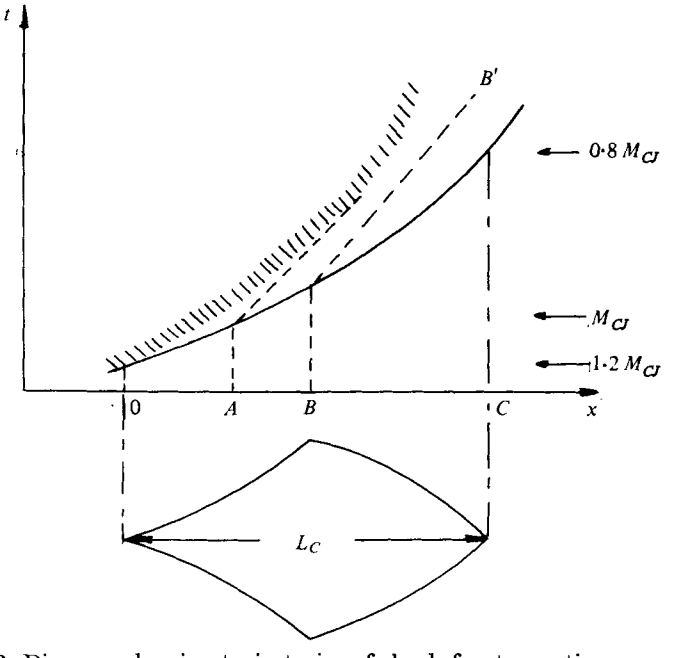

FIGURE 13. Diagram showing trajectories of shock front, reaction zone and particle path in a detonation cell.

We may, therefore, express the criteria for criticality for re-ignition in a diffracted wavefront as

$$\partial M_s/\partial y_s \lesssim \Delta M_{CJ}/L_c, \tag{12}$$

where ΔM_{CJ} lies in the range 0·1 to 0·2M_{CJ}. Before we can evaluate the above criterion the magnitude of the transverse velocity gradient along the length of diffracted shock front $\partial M_s/\partial y_s$ must be determined.

5. A theoretical model

5.1. *Whitham's theory of shock diffraction*

For our purpose the theory of Whitham (1957) for a diffracting shock wave around a corner of 90° angle will be used. In shock-ray coordinates the shock position is defined by $\alpha = a_0 t$ = constant, where a_0 is the sound speed in the undisturbed gas, while the ray position is given by β = constant. Near the shock front the lines β = constant can be identified with the particle paths. The nomenclature is defined in the diagram of figure 12. At the corner O the expansion is a simple wave (Prandtl–Meyer) and the positive C^+ characteristics are straight lines centred at the origin. Whitham's theory shows that the Mach number M is constant along each C^+ and the inclination $\theta(M)$ of the rays with respect to the x axis is constant along each C^+. This inclination is given by Whitham (1957) as

$$\theta(M) = n^{\frac{1}{2}}(\cosh^{-1} M - \cosh^{-1} M_0), \tag{13}$$

where $n = 2/K(M_1)$ where M_1 is the average value of M and M_0, and $K(M)$ is the slowly varying Chester function which is treated as a constant in Whitham's analysis. For $M_1 \to \infty$, $n = 5{\cdot}0743$. The relation between the ray-theory coordinates (α, β) and the shock-front cartesian coordinates (x_s, y_s) is defined by the equations given by Whitham (1957) and Skews (1967) as

$$\tan m = \frac{A\,d\beta}{M_0\,d\alpha} = \frac{1}{M_0}\left(\frac{M_0^2-1}{n}\right)^{\frac{1}{2}}, \tag{14}$$

where m is the angle between a C^+ and a ray, and A is the tube area. An alternative expression for m, in terms of γ and shock Mach number M_s, is given by Skews (1967):

$$\tan^2 m = (\gamma-1)(M_0^2-1)\{M_0^2 + 2/\gamma - 1\}/(\gamma+1)M_0^4. \tag{15}$$

From (14), by direct integration along a C^+ characteristic, we obtain

$$x_s = \frac{M_s \cos(\theta+m)}{\cos m}\alpha \quad \text{and} \quad y_s = \frac{M_s \sin(\theta+m)}{\cos m}\alpha. \tag{16}$$

5.2. *Expression of critical condition*

In § 4 we have stipulated a criterion for re-initiation to occur behind the attenuating shock front, by demanding that the transverse gradient of the Mach number, at any shock position α, must be less than the ratio $\Delta M_{CJ}/L_c$. For the range of Mach numbers that are of interest in detonations, the angle m is sensibly constant around the value of 23° (equation 14). Hence from (16) we have

$$\left(\frac{\partial M_s}{\partial y_s}\right)_\alpha = \frac{\cos m}{\alpha}\,\frac{[M_s^2-1]^{\frac{1}{2}}}{(M_s^2-1)^{\frac{1}{2}}\sin(\theta+m) + M_s n^{\frac{1}{2}}\cos(\theta+m)}. \tag{17}$$

Since we are interested in values of $(\partial M_s/\partial y_s)_\alpha$ at, or near, the head of the expansion wave, $M_s \simeq M_{CJ} \gg 1$. Hence in (17) we may approximate $(M_s^2-1)^{\frac{1}{2}}$ by M_s, giving

$$\left(\frac{\partial M_s}{\partial y_s}\right)_\alpha = \frac{\cos m}{\alpha}\,\frac{1}{\sin(\theta+m) + n^{\frac{1}{2}}\cos(\theta+m)}. \tag{18}$$

Using (16), α may be expressed in terms of the shock cartesian coordinate x_s:

$$\left(\frac{\partial M_s}{\partial y_s}\right)_{x_s} = \frac{M_s}{x_s}\frac{1}{[\tan(\theta+m)+n^{\frac{1}{2}}]}. \tag{19}$$

The condition for re-initiation may thus be obtained by combining (12) and (19) to give

$$\frac{M_s}{x_s}\frac{1}{[\tan(\theta+m)+n^{\frac{1}{2}}]} \lesssim \frac{\Delta M_{CJ}}{L_c}, \tag{20}$$

or

$$\frac{1}{[\tan(\theta+m)+n^{\frac{1}{2}}]} \lesssim \frac{1}{2}\left(\frac{x_s}{S}\right)\left(\frac{\Delta M_{CJ}}{M_{CJ}}\right), \tag{21}$$

since $L_c \simeq 2S$, where L_c and S are the cell length and spacing respectively. $\theta(M)$ is determined by (13) by writing M_{CJ} for M_0.

5.3 *Application of the criterion to the present results*

If the above model is valid then extinction of the diffracted portion of the detonation front occurs in the immediate vicinity of the area change because of the large value of the gradient $\partial M_s/\partial y_s$ there, with consequent production of non-reactive transverse waves. As the shock position coordinate x_s increases $\partial M_s/\partial y_s$ decreases and re-initiation will occur at some point along the generator of the wedge formed by the limiting C^+ characteristic when the inequality (8) is satisfied. For a given system and tube diameter the position of the re-ignition point moves further towards the apex of the wedge as the initial pressure is decreased.

It will be recalled that Mitrovanov & Soloukhin (1964) found that, at critical re-ignition in flat channels, the number of transverse waves across the diameter of the channel, for all oxyacetylene mixtures, is 10 (equation 5). Referring to figure 6 we can express this result as

$$(x_s/S)_{\text{exp.}} = 5\cot m. \tag{22}$$

Moreover, we have established in the present work that this condition holds at all points along the wedge. Referring to figure 6, re-ignition is shown to occur at C so that AB will contain 10 transverse waves; this result is not surprising since it merely expresses the similarity of the re-ignition process at C and D. Equation (22) thus expresses a generalized experimental result for all points along the wedge.

The present study has been restricted to stoichiometric acetylene–oxygen at different initial pressures so that M_{CJ} has remained almost constant with a value of approximately 7. It follows from (14) that the angle m has the constant value of approximately 23°. Substituting this value for m in (22) gives $(x_s/S)_{\text{exp.}} \simeq 10$. The predicted values for this ratio, $(x_s/S)_{\text{theor.}}$ by the criterion for critical re-initiation, expressed in (21), lie between 8 and 4, according to which value of ΔM_{CJ} is adopted; the upper value corresponds to $\Delta M_{CJ} = 0{\cdot}1 M_{CJ}$ and the lower value to $\Delta M_{CJ} = 0{\cdot}2 M_{CJ}$. Considering this lack of precision in specifying the value of ΔM_{CJ}, the agreement between the experimental and predicted values of (x_s/S) is very satisfactory, and confirms that the essential mechanism expressed by the criterion for criticality is correct. The model also suggests that the experimental result, $(x_s/S) \approx 10$, found for oxyacetylene waves, should apply to all detonative systems. This important generali-

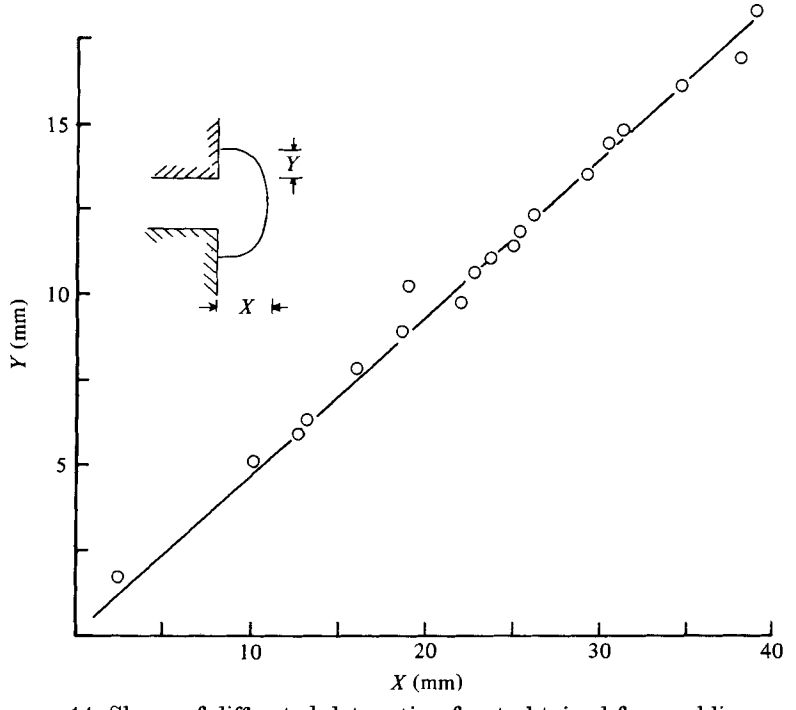

FIGURE 14. Shape of diffracted detonation front obtained from schlieren records.

zation remains to be investigated by further experimental work with other gaseous systems.

6. Discussion

The justification for using a simplified theory of non-reactive shock diffraction for the discussion of the behaviour of a detonation wave is based upon our observations of the shock front trajectories; these were derived from streak photographs and are plotted in figure 14. According to Whitham's theory the ratio of the undisturbed shock velocity to that along the wall is 0·5; this value agrees closely to that observed in figure 14 for a wave in a reactive gas. And since all the regions of gas-dynamical interest, as far as the transverse waves are concerned, lie very close to the shock front, the non-idealities that occur in the flow field at greater distances will not affect the conclusions derived from the model. Furthermore, although the CJ plane, at which the flow velocity is sonic with respect to the front, prevents longitudinal expansion waves from overtaking the front, no such restriction is placed on the transverse component of the expansion, which is solely of relevance to the model.

In § 1 reference was made to the work of Dremin & Trofimov (1965) on the critical diameters of liquid explosives. If the flow field, as shown in figure 15, is described in a frame of reference with origin fixed at A, the edge or boundary of the attenuating detonation wave, then the essence of the Dremin & Trofimov theory is as follows. A particle entering the shock front at A will react provided it is not engulfed by the head of the expansion BB' before it has completed the necessary residence time, τ_s,

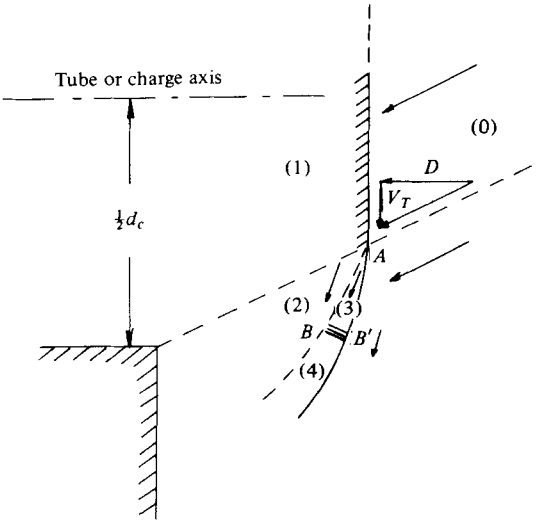

FIGURE 15. Diagram defining the nomenclature used in the discussion of the Dremin & Trofimov model.

for the induction reactions in region (3). The velocity of BB', relative to A, is $(U_3 - a_3)$, where U and a are the particle and sound velocities respectively, so that if t_1 is the time reaction takes place after entry of the particle,

$$(U_3 - a_3)\, t_1 = U_3 \tau_s. \tag{23}$$

Following reaction, a transverse detonation wave is formed in the shock-compressed gas (3). This detonation propagates both away from and towards A, reaching A after a further time interval t_2 given by

$$t_2 = U_3 \tau_s / (D_3 - U_3), \tag{24}$$

where D_3 is the velocity of a detonation in (3). At the critical diameter the transverse detonation must arrive at the tube axis in a time $(t_1 + t_2)$, given by

$$d_c = 2V_T(t_1 + t_2), \tag{25}$$

where V_T is the transverse velocity of A. Equations (23), (24) and (25) give the following expression for d_c:

$$d_c = 2U_3 V_T \tau_s \left[\frac{1}{(D_3 - U_3)} + \frac{1}{(u_3 - a_3)}\right]. \tag{26}$$

Dremin & Trofimov equate V_T to the velocity of the oblique transverse waves, which, on average, has the value a_{CJ}. The above model, although it differs in certain important details from the present one, recognizes that the basic mechanism is that of explosive re-initiation following the failure of the transverse waves. However its weakness lies in the assumption that region (3) is uniform and that τ_s is evaluated under steady-state one-dimensional conditions. This is clearly not valid and a realistic assessment of τ_s requires the flow details of the non-steady region (3) to be known. Substitution of steady-state values of τ_s in (26) are found to yield values of d_c, for the oxyacetylene system, which are between one and two orders of magnitude too small. The present

analysis avoids the difficulties encountered in the determination of the kinetics of non-steady flow by appealing to the behaviour of the induction zone behind the decaying shock front in an individual cell, and to the Shchelkin instability criterion. In addition the present model offers a qualitative explanation of Mitrovanov & Souloukhin's (1964) empirical observation that $d_c = 10S$ for a flat channel and $d_c = 13S$ for a circular tube. For the circular tube leading into a circular tank the effects of the expansion on the flow field behind the detonation will be much more severe (Sloan & Nettleton 1975, 1978).

7. Conclusions

Confirmation has been obtained of the experimental observation of Mitrovanov & Soloukhin that the critical width of a flat channel is ten times the equilibrium transverse wave spacing S in detonation waves in oxyacetylene mixtures. Additionally their observation of the difference between the wave behaviour in flat and circular channels is qualitatively explained.

For both critical and supercritical conditions re-ignition occurs at sites along the head of the expansion wave originating at the area change. Furthermore if x_s is the shock position at re-ignition then (x_s/S) is invariant and equal to $5\cot m$, where m is the angle between the head of the expansion wave and the tube axis.

By equating the velocity gradient of the shock front, which is approximately $\Delta M_{CJ}/L_c$, with that of a non-reactive diffracted shock derived by Whitham's theory, a criterion for criticality is established. The predictions of the criterion are in good agreement with observation.

The present analysis is in broad agreement with the underlying principles of the Dremin & Trofimov theory of critical diameters. However, it avoids the difficulties that are inherent in the latter by not making steady-state assumptions regarding the flow field behind the diffracted shock.

REFERENCES

Barthel, H. O. 1974 Predicted spacings in hydrogen–oxygen–argon detonations. *Physics Fluids* **17**, 1547.

Bull, D. C., Elsworth, J. E., Hooper, G. & Quinn, C. P. 1976 A study of spherical detonation in mixtures of methane and oxygen diluted by nitrogen. *J. Phys.* (D: Appl. Phys.) **9**, 1991.

Dremin, A. N. & Trofimov, V. A. 1965 On the nature of the critical diameter. *Tenth Symposium (International) on Combustion*, p. 839. The Combustion Institute.

Edwards, D. H., Hooper, G., Morgan, J. M. & Thomas, G. O. 1978 The quasi-steady regime in critically initiated detonation waves. *J. Phys.* (D: Appl. Phys.) **11**, 2103.

Gvozdeva, L. G. 1961 *Prŷkl. Mekh.* **33**, 731.

Mitrovanov, V. V. & Soloukhin, R. I. 1964 The diffraction of multifront detonation waves. *Soviet Phys. Dokl.* **9**, 1055.

Shchelkin, K. I. 1959 Two cases of unstable combustion. *Soviet Phys. JETP* **9**, 416.

Skews, B. W. 1967 The shape of a diffracting shock wave. *J. Fluid Mech.* **29**, 297.

Soloukhin, R. I. & Ragland, K. W. 1969 Ignition processes in expanding detonations. *Combust. Flame* **13**, 295.

Sloan, S. A. & Nettleton, M. A. 1975 A model for the axial decay of a shock wave in a large abrupt area change. *J. Fluid Mech.* **71**, 769.

SLOAN, S. A. & NETTLETON, M. A. 1978 A model for the decay of a wall shock in a large abrupt area change. *J. Fluid Mech.* **88**, 259.

STREHLOW, R. A. & ENGEL, C. D. 1969 Transverse waves in detonations. II. Structure and spacing in H_2–O_2, C_2H_2–O_2, and CH_4–O_2 systems. *A.I.A.A. J.* **7**, 492.

STREHLOW, R. A. 1970 Multidimensional detonation wave structure. *Astronautica Acta* **15**, 345.

SUBBOTIN, V. A. 1974 Two kinds of transverse wave structures in multifront detonation. *Fiz. Goreniya i Vzryva*, II, no. 1, 96.

THOMAS, G. O. 1979 Gasdynamic studies of diverging detonations. Ph.D. dissertation, University of Wales.

URTIEW, P. A. 1975 From cellular structure to failure waves in liquid detonations. *Combust. Flame* **25**, 241.

VASILIEV, A. A., GAVRILENKO, T. P. & TOPCHIAN, M. E. 1972 On the Chapman–Jouguet surface in multiheaded gaseous detonations. *Astronautica Acta* **17**, 499.

WHITE, D. R. 1967 Density induction times in very lean mixtures of D_2, H_2, C_2H_2 and C_2H_4 with O_2. *Eleventh Symposium (International) on Combustion*, p. 147. The Combustion Institute.

WHITHAM, G. B. 1957 A new approach to problems of shock dynamics. Part I. Two-dimensional problems. *J. Fluid Mech.* **2**, 145.

ZELDOVICH, Y. B., KOGARKO, S. M. & SIMONOV, N. N. 1956 An experimental investigation of spherical detonation in gases. *Soviet Phys. tech. Phys.* **1**, 1689.

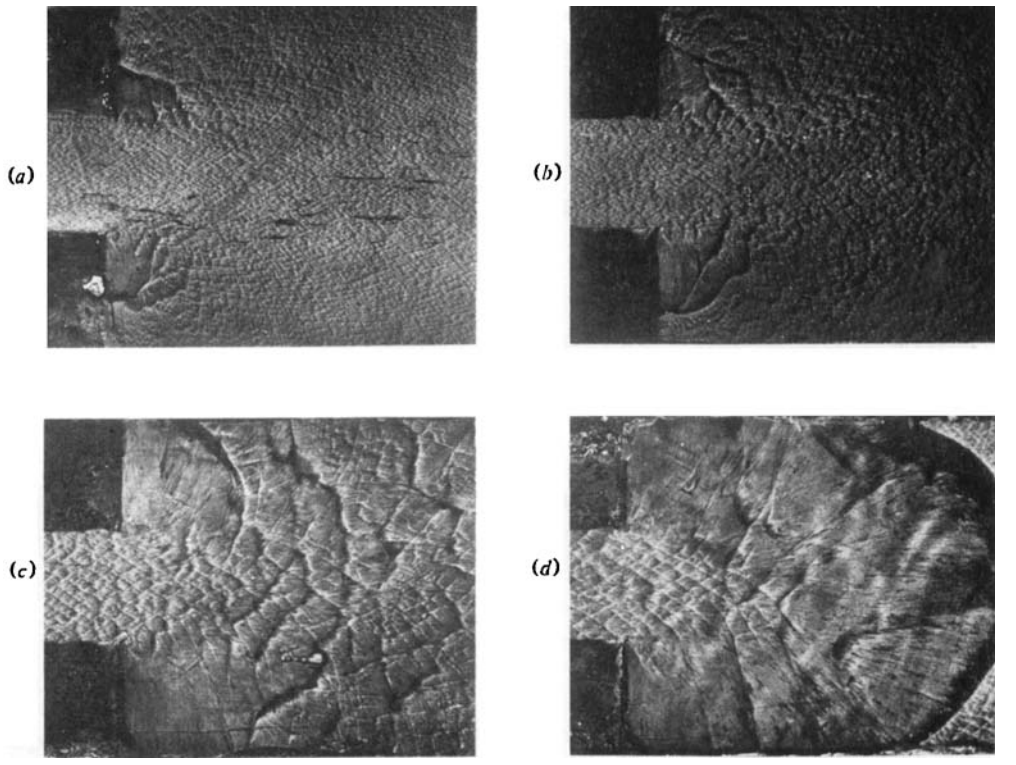

FIGURE 5. Smoked-foil records obtained with stoichiometric oxyacetylene at different initial pressures, p_0: (*a*) 180 Torr and (*b*) 150 Torr, supercritical wave; (*c*) 110 Torr critical wave, and (*d*) 60 Torr, failing wave.

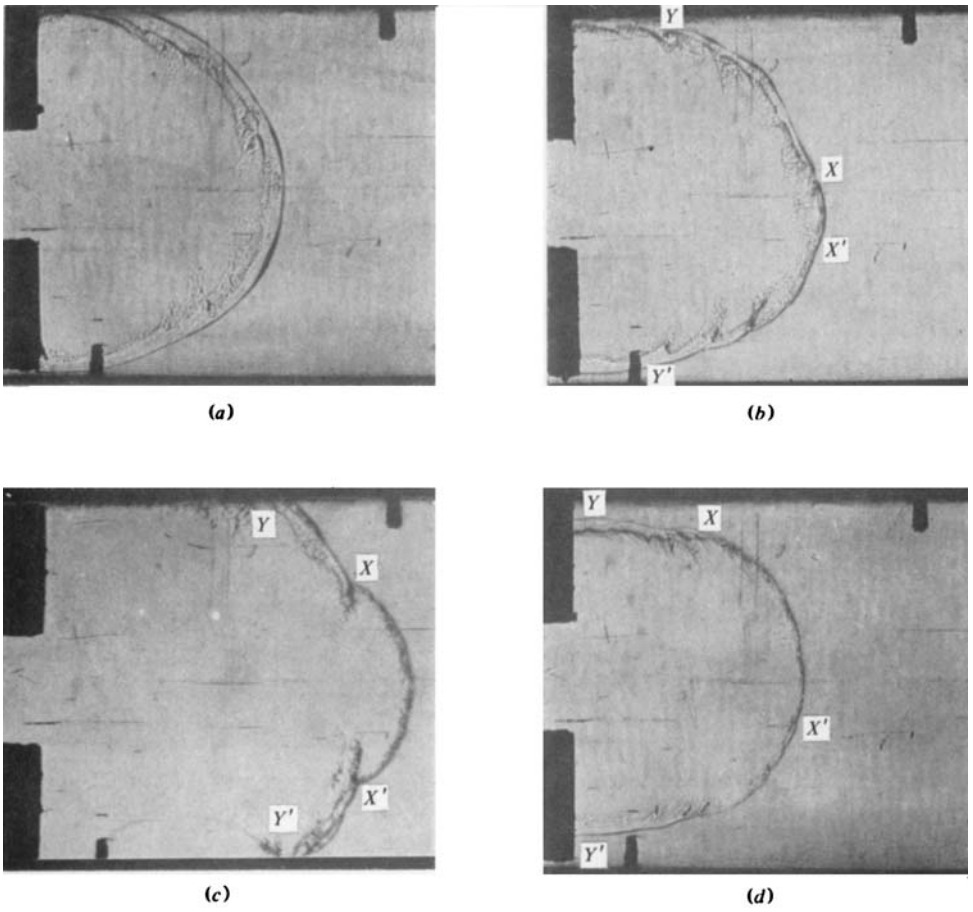

FIGURE 8. Spark schlieren photographs in stoichiometric oxyacetylene waves. (*a*) 60 Torr, (*b*) and (*c*) 110 Torr and (*d*) 150 Torr.

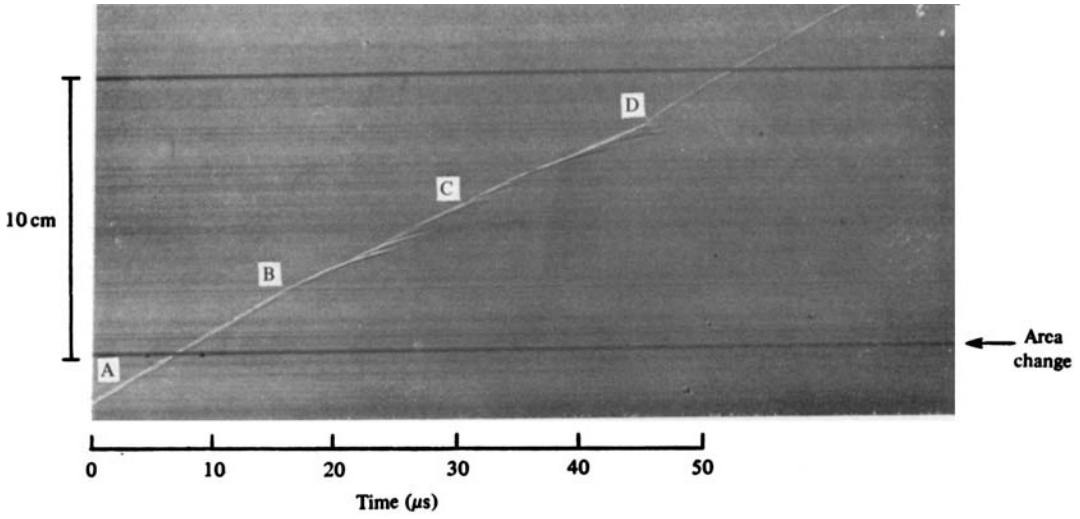

FIGURE 10. Streak schlieren photograph obtained with stoichiometric oxyacetylene under critical conditions.